AIAA 2000-0890

# DEVELOPMENT OF A DESIGN METHODOLOGY FOR RECONFIGURABLE FLIGHT CONTROL SYSTEMS

R. A. Hess and C. McLean
Dept. of Mechanical and Aeronautical Engineering
University of California
Davis, CA

**38th Aerospace Sciences Meeting & Exhibit**
10-13 January 2000 / Reno, NV

# Development of a Design Methodology for Reconfigurable Flight Control Systems

R. A. Hess[1] and C. McLean[2]
Dept. of Mechanical and Aeronautical Engineering
One Shields Ave.
University of California
Davis, CA 95616-5294

## Abstract

A methodology is presented for the design of flight control systems that exhibit stability and performance robustness in the presence of actuator failures. The design is based upon two elements. The first element consists of a control law that will ensure at least stability in the presence of a class of actuator failures. This law is created by inner-loop, reduced-order, linear dynamic inversion, and outer-loop compensation based upon Quantitative Feedback Theory. The second element consists of adaptive compensators obtained from simple and approximate time-domain identification of the dynamics of the "effective vehicle" with failed actuator(s). An example involving the lateral-directional control of a fighter aircraft is employed both to introduce the proposed methodology and to demonstrate its effectiveness and limitations.

## Introduction

The ability of an aircraft to survive with failed or damaged actuation systems is an important consideration for safety of flight. The accommodation of such failures is typically sought through reconfigurable or adaptive control systems. Many examples of research in this area can be found in the literature, e.g., Refs. 1-5. The work to be described herein builds upon a design methodology introduced in Ref. 5. The fundamental philosophy of that work was that an adaptive/reconfigurable design should be an integral part of a robust flight control methodology. This philosophy allows the nominal flight control system to share a considerable part of the responsibility for performance recapture when actuators are damaged or fail and allows the adaptive system time for identification and reconfiguration.

The work or Ref. 5 dealt with a single-input, single-output (SISO) system involving a longitudinal flight control design with redundant effectors. The nominal flight control system was based upon a Quantitative Feedback Theory design emulated by a simplified Pre-Design Technique (PDT) described in Ref. 6. The adaptive logic was implemented as an iterative gain adjustment in the single PDT compensator. While effective in improving performance in the presence of a class of actuator failures, the adaptive technique suffered from long convergence times during which the pilot was excluded from control. This deficiency eliminated this approach for consideration for multi-input, multi-output (MIMO) designs. The work to be described herein will attempt to remove this limitation and to provide a more powerful adaptive technique than simple gain adjustment.

## Reconfiguration Methodology

The reconfiguration approach to be discussed involves an approximate, time-domain identification of the dynamics of the "effective vehicle" where the term "effective" implies that the nominal flight control law remains in operation. The identification produces input-response transfer functions and is accomplished while the pilot is excluded from active control. After identification, additional outer control

---

[1]Prof. and Vice Chairman, Associate Fellow AIAA
[2]Graduate Student; Currently Project Engineer, DST Controls, Benicia, CA

loops are enabled that utilize compensation elements derived from the identified effective vehicle dynamics. No additional sensor requirements are encountered as the outer-loop feedback variables are the vehicle response variables already used by the PDT compensation elements. Immediately after enabling these loops, control is returned to the pilot. The philosophy behind this approach is to simplify the reconfiguration as much as possible, and to leave the nominal flight control system undisturbed so as to preserve its robustness. The latter is an important consideration in minimizing the trim upsets that may accompany certain actuator failures, e.g., non-null failures. Note that if the actuator failures involve nonlinearities that are encountered in the step test inputs, their effects will be reflected in the resulting control adaptive compensation. For example, an actuator failure that causes a significant reduction in the device's rate-limits may result in an additional apparent time delay in the vehicle's step response.[7] As will be seen, this delay is one of the parameters estimated in the identification procedure. As in Ref. 5, it is assumed that redundant controls are in evidence, i.e., in any control loop subject to reconfiguration, at least two effectors are involved in the control of each outer-loop response variable.

## Example

From a tutorial standpoint the design methodology is best described through an example. This will involve the design of a lateral-directional flight control system for a simple model of the former NASA High-Angle of Attack Research Vehicle (HARV). This model was chosen since model details and the nominal control system design are available in the literature.[8,9,10] The vehicle is shown in Fig. 1 with the five control effectors employed in the control law. In the design discussed in Ref. 10, the linear, dynamic inversion was gain scheduled for 18 flight conditions. For the purposes of exposition, only a single flight condition will be utilized herein. This condition is Mach No. = 0.6, Altitude = 20,000 ft. The flight control system configuration is shown in Fig. 2. Figure 3 summarizes the steps in the design methodology to be described.

### Define Flight Conditions

The linear dynamic inversion control law, as described in Ref. 10 was gain-scheduled over 18 flight conditions, ranging from Mach No. = 0.2, Alt. = 10,000 ft to Mach No. = 0.9, Alt. = 30,000 ft. Table 1 gives the dynamics of the simplified vehicle model for the single flight condition discussed herein. Also listed are the dynamics of the five actuators, including amplitude and rate limits.

### Design Reduced-Order, Linear Dynamic Inversion Laws

Since the dynamic inversion here is reduced-order, full-state feedback including actuator states is not required.[9] Feedback of only rigid body states, roll-rate $p$, yaw-rate $r$, and sideslip beta is required. The inversion law provides an approximately decoupled control law with first-order-like command-response characteristics. In this formulation, roll control is about the velocity vector. As the name implies the control distribution matrix in Fig. 2 distributes the two pseudo control commands to the five actuators. This matrix is implemented with only a single non-zero element in any row. The non-zero element is proportional to the rate limit of the actuator that it affects. As seen in Table 1, the control distribution matrix selects aileron, differential tail and roll thrust vectoring for control of roll-rate, and rudder and yaw-thrust vectoring for control of sideslip. If desired, this definition allows use of the "software rate limiters" discussed in Ref. 11. For simplicity, these limiters were not included in the present study.

### Define Actuator Failure Class

The class of actuator failures is shown in Table 2. As can be seen, 30 failures were included, with 28 of the failures defined as a gain reduction and/or time delay addition to the linear actuator description(s), one including a biased control surface position and one involving a failure with a 95% reduction in actuator rate limits. While the gain reductions model loss of actuator effectiveness, the inclusion of pure time delays is admittedly somewhat artificial. However, these failure modes were included to provide both amplitude and phase variations in the frequency-domain description of the actuators.

### Design QFT/PDT Compensators and Prefilters

After the dynamic inversion laws were created, the QFT/PDT compensators were obtained. The purpose of these compensators was to provide stability and performance robustness for the nominal vehicle (no actuator failures) across the flight

envelope and to provide at least stability robustness for cased in which actuator failures occurred. Although actuator failures, *per se*, were not included in the study of Ref. 10, model uncertainty was introduced in the formulation by creating 10 additional vehicle models at each flight condition. These additional models were obtained by perturbing the stability derivatives in the nominal configuration by a maximum of 20%. The QFT/PDT diagonal compensation matrix was then obtained by the loop shaping procedure described in Ref. 6. These compensation elements are given by

$$G_{QFT}(1,1) \approx \frac{\omega_{c_1}}{s} \cdot \frac{1}{(\beta/\nu_\beta)_{nom}} \cdot \frac{1}{\left(\frac{s}{15\omega_{c_1}}+1\right)^{\gamma_1}} \quad (1)$$

$$G_{QFT}(2,2) \approx \frac{\omega_{c_2}}{s} \cdot \frac{1}{(p/\nu_p)_{nom}} \cdot \frac{1}{\left(\frac{s}{15\omega_{c_1}}+1\right)^{\gamma_2}}$$

where $\nu_\beta$ and $\nu_p$ are the first and second inputs to the dynamic invertor as shown in Fig. 2 and $\gamma_1$ and $\gamma_2$ represent the excess poles over zeros of $(\beta/\nu_1)_{nom}$ and $(p/\nu_2)_{nom}$, respectively. The relations of Eqs. 1 ensure that the well-known, desirable frequency domain attributes of a loop transmission will be in evidence in each of the (approximately) decoupled control loops of Fig. 2.[12] No changes in the resulting compensator matrix $G_{QFT}(s)$ were required to accommodate the 30 linear failures of Table 2, for the single flight condition considered here. This assessment was based upon actuators with no amplitude or rate limitations. Of course, the ability of the reconfiguration scheme to handle any of the failures with rate and amplitude limited actuators (healthy or failed) had to be ascertained through the computer simulation to be described. The diagonal elements of the prefilter matrix shown in Fig. 2 were created to provide acceptable handling qualities for the nominal vehicle across the 18 flight conditions using the predictive methodology introduced in Ref. 13.

The bode diagrams of the transfer functions between command and response variables for the vehicle with damaged actuators are shown in Figs. 4-7 for all but Configs. 30-31 where nonlinearities or control offsets are involved. As the figures indicate, significant variations in the vehicle dynamics have been introduced by the class of actuator failures.

**Formulate Identification Logic**

The identification of the "effective vehicle" with both the dynamic inversion controller and the QFT/PDT controllers in place was accomplished by applying successive test inputs in the beta and *p* loops as shown in Fig. 2. The identification is predicated on the step response. The test inputs for this example are shown in Fig. 8. A doublet is used for the *p* loop to bring the aircraft back to the approximate roll attitude that existed when the reconfiguration began. The identification logic was kept as simple as possible herein. This approach will attempt to capitalize on the fact that the action of the dynamic inversion and PDT control laws will allow the transient responses (linear or nonlinear) to the test inputs to be fitted with a pair of relatively simple, lower-order models, characterizing either an *underdamped*, or *overdamped* response. These models are defined as

**Underdamped-type responses**

$$(\hat{\beta}/\beta_c) \text{ or } (\hat{p}/p_c) = \frac{K\omega_n^2}{z} \cdot \frac{(s+z)e^{-\tau_d s}}{s^2+2\zeta\omega_n s+\omega_n^2} \quad (2)$$

**Overdamped-type responses**

$$(\hat{\beta}/\beta_c) \text{ or } (\hat{p}/p_c) = K\omega_n^2 \frac{e^{-\tau_d s}}{s^2+2\zeta\omega_n s+\omega_n^2} \quad (3)$$

The parameters of the model of Eqs. 2 and 3 are estimated from the transient responses as indicated in Fig. 9 and 10. The "gain" $K$ was not estimated but was always assumed to be unity. This assumption is justified since the PDT compensation always provides at least a type "1" system, i.e. at least one pole at the origin of the loop transmissions $\beta/e_\beta$ and $p/e_p$ in Fig. 2. This in turn guarantees zero steady-state error to the test step input. Although not pursued in this example, the effects of any turbulence or sensor noise on the step responses can be lessened by the common practice of filtering the responses recorded off-line, first in forward time, then in reverse time. This process effectively removes any lags in the filtered responses due to filtering. It should also be noted that the $\tau_d$ identified as in Figs.

9 and 10 can accommodate the "reverse action" associated with high frequency (above crossover) non-minimum phase zeros in the damaged vehicle response. It should also be noted that the model fits above may give relative poor matches to the actual vehicle time responses but still yield an acceptable reconfigurable compensator. Although approximate and simple in form, the identification logic has the advantage of requiring little computational effort. In addition, the effects of nonlinear failed-actuator behavior, if encountered in the test step inputs, will be reflected in the adaptive compensation. Finally, it is obvious that other more sophisticated schemes can be for identification.

**Create Adaptive, Outer-Loop Compensators**

The outer loop compensators $G_\beta(s)$ and $G_p(s)$ are created as follows:

$$G_{\beta\text{-}RC} = \frac{\omega_{c_\beta}}{s} \cdot \frac{1}{\left(\hat{\beta}/\beta_c\right)_{nd}} \cdot (\tau_d s+1)$$

$$G_{p\text{-}RC} = \frac{\omega_{c_p}}{s} \cdot \frac{1}{\left(\hat{p}/p_c\right)_{nd}} \cdot (\tau_d s+1) \qquad (4)$$

Here, $\left(\hat{\beta}/\beta_c\right)_{nd}$ and $\left(\hat{p}/p_c\right)_{nd}$ refer to the dynamics identified from Eqs. (2) or (3) with the time delay removed and padded with extra high-frequency zeros so that both $\left(\hat{\beta}/\beta_c\right)_{nd}$ and $\left(\hat{p}/p_c\right)_{nd}$ contain two more zeros than poles. The lead term $(\tau_d s+1)$ is included to reduce the phase lags attributable to the time delay $\tau_d$. To ensure adequate stability margins, the crossover frequencies for each of the outer loops were chosen initially as

$$\omega_c = \min_{\omega_c}[2.0,\ 0.5/\tau_d] \qquad (5)$$

The crossover frequency so obtained is an estimate, since it is based upon an exact cancellation of the vehicle dynamics by those estimated from the identification procedure. Just as in the case of the QFT/PDT compensators, the adaptive, outer-loop compensation ensures that the well-known, desirable frequency-domain attributes of a loop transmission will be in evidence in each of the (approximately) decoupled control loops of Fig. 2.

**Simulation**

A computer simulation of the reconfigurable control system was conducted. The simulation involved models of compensatory pilot behavior in the beta and $p$ loops as described in Ref. 13. The pilot models are given in Table 3 along with the assumed dynamics of the cockpit force/feel systems for the lateral stick (providing roll-rate command $p_c$) and rudder pedals (providing sideslip command $\beta_c$). With the nominal (undamaged) aircraft, the pilot models of Table 3 yielded crossover frequencies of 1.5 rad/sec in each loop. A block diagram representation of the pilot/vehicle system is shown in Fig. 11. No changes in the pilot dynamics were allowed after failure or reconfiguration.

The scenario for pilot-in-the-loop reconfiguration went as follows:

1.) A failure is detected. The detection logic is beyond the scope of this study. No isolation or identification of the particular actuator(s) affected is assumed.

2.) Pilot inputs are removed from the system and a 5 sec quiescent period follows to allow transients to die out.

3.) The test inputs of Fig. 8 are employed. The p-loop is reconfigured first and the reconfigured p-loop compensator is brought on-line at the completion of the 10 sec doublet. Time for identification and reconfiguration was considered negligible and ignored. After the doublet was completed, another 5 sec quiescent period is employed. The beta-loop is reconfigured next. Note that the beta loop dynamics are identified and reconfigured with the reconfigured $p$ loop in operation. The reconfigured beta-loop is brought on line immediately at the conclusion of the 5 sec beta-test pulse. Selection of loop closure sequence was based upon the fact that the beta loop is serviced by only two actuators, and reconfiguration of the p loop would reduce the demands upon the remaining healthy actuator in the beta loop should one of them have failed.

4.) A third, 5 sec quiescent period is employed after which control is returned to the pilot. The entire reconfiguration time is thus 30 sec.

The design summary of Figure 3 indicates some iterative modification of the adaptive, outer-loop compensation may be necessary. Here these modifications consisted of the following:

a.) The crossover frequency logic of Eq. 5 for the beta loop was changed to

$$\omega_{c_\beta} = \min_{\omega_c}[1.0,\ 0.5/\tau_d] \qquad (6)$$

Lowering the constant from 2 in Eq. 5 to 1 in Eq. 6 led to better reconfigured performance, a fact attributable to the relatively simple approximation for the overdamped response types that dominated the beta responses to the beta test input.

b.) Logic was incorporated to prevent adaptation in those instances in which the robustness of the dynamic inversion law and the QFT/PDT controller provided sufficient performance robustness. The logic for each loop was as follows: For underdamped responses, if the overshoot was less than or equal to 5%, no reconfiguration was undertaken; for overdamped response, if the 2% settling time was less than or equal to 4 sec, no reconfiguration was undertaken.

**Results**

As Fig. 11 indicates, in evaluating the reconfiguration design, a roll-attitude command was given to the pilot. This random appearing command was obtained as the sum of five sinusoids and produced a signal with an root-mean-square (RMS) value of 10 deg. Although no beta command was provided, the pilot was assumed to be actively attempting to null beta errors caused by inevitable dynamic cross-coupling from the roll-attitude control activity.

One instability was obtained in simulation of the 30 actuator failure cases. This was Config. 13. In this case, no reconfiguration occurred. The instability was traced to the effects of actuator saturation. The effects of this saturation were not included in the original stability study that created the PDT compensators. Thus, this failure would have to be removed from the actuator failure class. Of the 30 failures, nine resulted in no reconfiguration being attempted in either loop, six resulted in reconfiguration in both loops, with the remaining 15 resulting in reconfiguration in one loop only and 13 of these 15 involved reconfiguration in the beta loop.

Space does not permit a discussion of each of the failures. In general, performance was improved in all cases where at least one of the loops reconfigured. Two challenging failures can be selected for presentation however, Configs. 9 and 31. First, Figs. 12 and 13 show the tracking performance of the pilot/vehicle system with the nominal vehicle (Config. 1). Note that the higher frequency sinusoids in the roll command input provide a challenging tracking task. Figures 14 and 15 compare the roll and beta tracking with and without reconfiguration for Config. 9 where no reconfiguration occurred in the beta loop but did occur in the p-loop. Both figures show significant improvement in tracking performance. Figures 15 and 16 compare the roll and beta tracking with and without reconfiguration for Config. 31, where reconfiguration occurred in both loops. The most significant performance improvement is seen to come in the beta-loop tracking. This is in spite of the fact that a roll-control actuator (aileron) was the failed device. Figure 18 shows the 5 deg/sec aileron rate limiting occurring after reconfiguration.

The price to be paid for the simplicity of the lower-order models of Eqs. 2 and 3 is, of course, modeling errors. As an example, Figs. 19 and 20 show "identified" and "failed" vehicle models for a particular configuration. To allow meaningful comparison, all actuator limitations were removed. As can be seen, the lower-order models provide a relatively poor approximation to the actual, higher-order failed vehicle dynamics. However, it must be emphasized that system identification, *per se*, is not the goal of the methodology but is rather an intermediate step in establishing the dynamics of outer-loop compensators to improve system performance. Relatively poor frequency-domain matches can still provide acceptable plant inverse models for defining these compensators.

**Discussion**

The application of the proposed methodology to a simple aircraft model produces results superior to the methodology presented in Ref. 5. In that study, a SISO model of the longitudinal dynamics of the same aircraft at the same flight condition was employed. However, no inverse dynamic controller was used and only a single, inner-loop control was in

evidence based upon the QFT/PDT approach. SISO reconfiguration times averaged 25 sec, with the longest being 68 sec. In the present MIMO example, all reconfigurations were completed in 30 sec.

The 30 sec reconfiguration time was deliberately selected as conservative in the present study. An examination of the vehicle responses to the pulsive step inputs indicates that the 5 sec test input duration can probably be halved as can the 5 sec "quiescent" periods. Nonetheless, a lower limit of approximately 15 sec is the most one can probably achieve.

Of primary importance in improving the methodology is increasing the quality of the procedure used to identify the dynamics of the effective vehicle with failed actuator(s). A first step would include an increase in the order of the models of Eqs. 2 and 3. The consequence of this order increment (and concomitant increment in accuracy) would be an increase in the maximum allowable crossover frequency in each reconfigured loop.

## Conclusions

A flight control reconfiguration methodology based upon a two-element design approach has proved feasible in a limited evaluation. The methodology can accommodate significant and multiple actuator failures and requires no additional sensor requirements. The primary limitation of the technique is the requirement of eliminating pilot inputs while identification/reconfiguration is occurring. A significant improvement in the performance of the reconfigured system may be possible with a more sophisticated identification algorithm.

## Acknowledgement

This research was supported by a grant from NASA Langley Research Center. The grant technical manager is Dr. Barton Bacon.

## References

[1]Horowitz, I., "A Quantitative Inherent Reconfiguration Theory for a Class of Systems," *International Journal of Systems Science*, Vol. 16, No. 11, 1985, pp. 1377-1390.

[2]Ochi, Y., and Kanai, K., "Design of Restructurable Flight Control Systems Using Feedback Linearization," *Journal of Guidance, Control, and Dynamics*, Vol. 14, No. 5, 1991, pp. 903-911.

[3]Heiges, M., "Reconfigurable Controls for Rotorcraft," *Journal of the American Helicopter Society*, Vol. 42, No. 3, 1997, pp. 254-263.

[4]Burken, J., Lu, P. and Wu, Z., "Reconfigurable Flight Control Designs wiht Application to the X-33 Vehicle, AIAA Paper No. 99-4134, AIAA Guidance, Navigation and Control Conference, Portland, OR, 9-11 Aug., 1999.

[5]Hess, R. A., Siwakosit, W., and Chung, J., "Accommodating a Class of Actuator Failures in Flight Control Systems," *Journal of Guidance, Control, and Dynamics*, to appear.

[6]Henderson, D. K., and Hess, R. A., "Approximations for Quantitative Feedback Theory Designs," *Journal of Guidance, Control, and Dynamics*, Vol. 20, No. 4, 1997, pp. 828-831.

[7]Klyde, D. H., McRuer, D. T. and Myers, T. T., "Pilot-Induced Oscillation Analysis and Prediction with Actuator Rate Limiting," *Journal of Guidance, Control, and Dynamics*, Vol. 20, No. 1, 1997, pp. 81-90.

[8]Adams, R. J., Buffington, J. M., Sparks, A. G. and Banda, S. S. "An Introduction to Multivariable Flight Control Design," WL-TR-92-3110, Wright-Patterson AFB, OH, Oct. 1992.

[9]Snell, S. A., "Decoupling Control Design with Applications to Flight," *Journal of Guidance, Control, and Dynamics*, Vol. 21, No. 4, 1998, pp. 647-655.

[10]Siwakosit, W., Snell, S. A., and Hess, R. A., "Robust Flight Control Design With Handling Qualities Constraints Using Scheduled Linear Dynamic Inversion and Loop-Shaping," *IEEE Transactions on Control Systems Technology*, to appear.

[11]Snell, S. A., and Hess, R. A., "Robust, Decoupled, Flight Control Design with Rate Saturating Actuators," *Journal of Guidance, Control, and Dynamics*, Vol. 21, No. 3, 1998, pp. 361-367.

[12]Maciejowski, J. M., *Multivariable Feedback Design*, Addison Wesley, NY, 1989, Chap. 1.

[13]Hess, R. A., "A Unified Theory for Aircraft Handling Qualities and Adverse Aircraft-Pilot Coupling," *Journal of Guidance, Control, and Dynamics*, Vol. 20, No. 6, 1997, pp. 1141-1148.

**Table 1 Nominal Vehicle Model**

*Nominal Flight Condition: Alt. = 20,000 ft Mach No. = 0.6*

$$\dot{x}_r(t) = A_r x_r(t) + B_r u(t)$$

$$x_r(t) = [\beta(t) \quad p(t) \quad r(t)]^T$$

$$u(t) = [\delta_{DT} \; \delta_A \; \delta_R \; \delta_{RTV} \; \delta_{YTV}]^T$$

$$A_r = \begin{bmatrix} -0.166 & 0.0629 & -0.9971 \\ -12.97 & -1.761 & 0.5083 \\ 3.191 & -.01417 & -0.1529 \end{bmatrix}$$

$$B_r = \begin{bmatrix} -0.0142 & -0.00686 & 0.01851 & 0 & 0.005817 \\ 14.38 & 16.76 & 1.316 & 0.7007 & 0.0402 \\ 0.3389 & -0.385 & -1.051 & -0.004475 & -0.5511 \end{bmatrix} \begin{bmatrix} 0 & 0.6 \\ 0 & 1.0 \\ 1.0 & 0 \\ 0 & 0.6 \\ 0.6 & 0 \end{bmatrix}^a$$

*Actuator Descriptions*

| | | *amplitude limit* | *rate limit* |
|---|---|---|---|
| *differential tail* : | $\frac{30^2}{s^2+42.4s+30^2}$ | ±17.5 *deg* | 60 *deg/s* |
| *aileron*: | $\frac{75^2}{s^2+88.5s+75^2}$ | ±27.5 *deg* | 100 *deg/s* |
| *rudder* : | $\frac{72^2}{s^2+99.4s+72^2}$ | ±30 *deg* | 100 *deg/s* |
| *roll/yaw thrust*: | $\frac{20^2}{s^2+24s+20^2}$ | ±30 *deg* | 60 *deg/s* |

[a] Control distribution matrix $K$ included here with nonzero elements proportional to rate limits on actuators.

**Table 2 Actuator Failures**

| Failure No. | Actuator(s) | Failure Description |
|---|---|---|
| 1 | none | healthy aircraft |
| 2 | differential tail | complete failure (gain=0) |
| 3 | differential tail | gain reduction (gain=0.5) |
| 4 | differential tail | gain reduction (gain=0.5) + time delay (delay=0.4sec) |
| 5 | differential tail | time delay (delay=0.4sec) |
| 6 | aileron | complete failure (gain=0) |
| 7 | aileron | gain reduction (gain=0.5) |
| 8 | aileron | gain reduction (gain=0.5) + time delay (delay=0.4sec) |
| 9 | aileron | time delay (delay=0.4sec) |
| 10 | rudder | complete failure (gain=0) |
| 11 | rudder | gain reduction (gain=0.5) |
| 12 | rudder | gain reduction (gain=0.5) + time delay (delay=0.4sec) |
| 13 | rudder | time delay (delay=0.4sec) |
| 14 | roll thrust | complete failure (gain=0) |
| 15 | roll thrust | gain reduction (gain=0.5) |
| 16 | roll thrust | gain reduction (gain=0.5) + time delay (delay=0.4sec) |
| 17 | roll thrust | time delay (delay=0.4sec) |
| 18 | yaw thrust | complete failure (gain=0) |
| 19 | yaw thrust | gain reduction (gain=0.5) |
| 20 | yaw thrust | gain reduction (gain=0.5) + time delay (delay=0.4sec) |
| 21 | yaw thrust | time delay (delay=0.4sec) |
| 22 | yaw thrust + diff tail | complete failure of both (gains=0) |
| 23 | rudder + diff tail | complete failure of both (gains=0 |
| 24 | yaw thrust + aileron | complete failure of both (gains=0 |
| 25 | rudder + aileron | complete failure of both (gains=0) |
| 26 | yaw and roll thrust | complete failure of both (gains=0) |
| 27 | rudder + roll thrust | complete failure of both (gains=0) |
| 28 | roll thrust + aileron | complete failure of both (gains= |
| 29 | aileron + diff tail | complete failure of both (gains=0) |
| 30 | aileron | complete failure (gain=0) + 2.5 deg offset |
| 31 | aileron | gain reduction (gain=0.5) + time delay (delay=0.4 sec) + 5 deg/sec aileron rate limit |

**Table 3 Pilot Models**

beta-loop

$$Y_{p_\beta} = \frac{6.84 \cdot 10^4 (s+1) e^{-0.2s}}{s(s+2)[s^2+2(0.15)28.2s+28.2^2](s+39)}$$

p-loop

$$Y_{p_\phi} = \frac{2.6 \cdot 10^5 e^{-0.2s}}{[s^2+2(0.15)14.1s+14.1^2][s^2+2(0.78)28.9s+28.9^2]}$$

Pilot models contain force/feel system dynamics defined as

$$\frac{25^2}{[s^2+s(0.707)25s+25^2]}$$

All units normalized in pilot/vehicle system

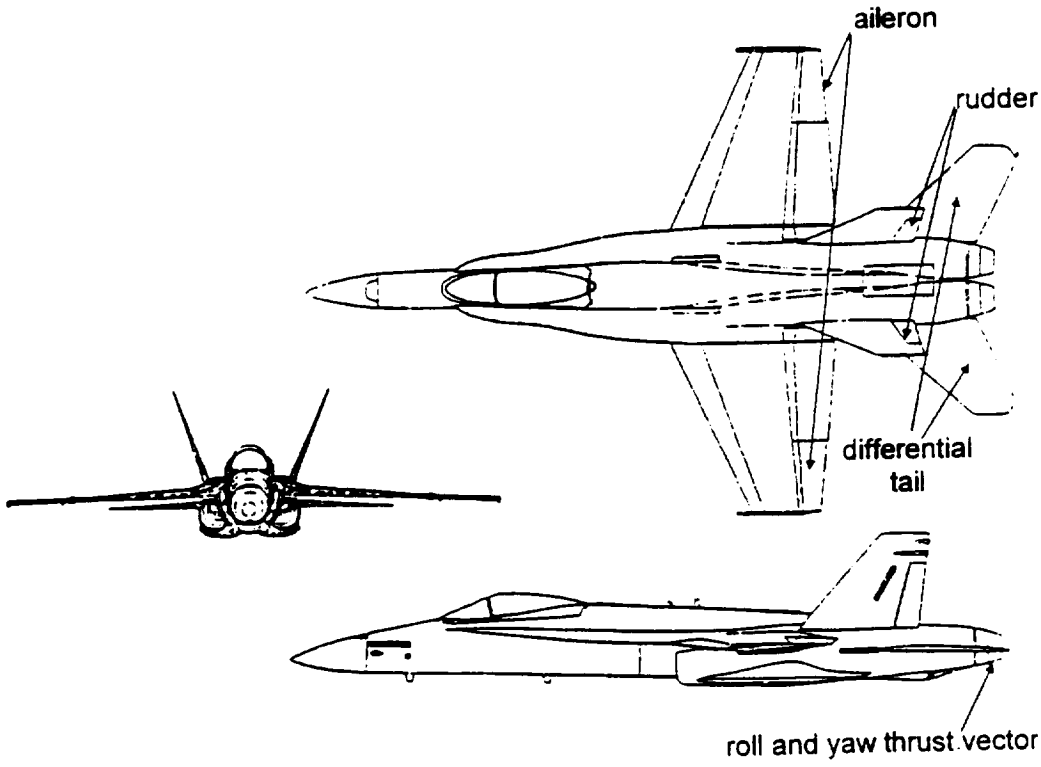


Figure 1 The NASA HARV with lateral-directional control effectors

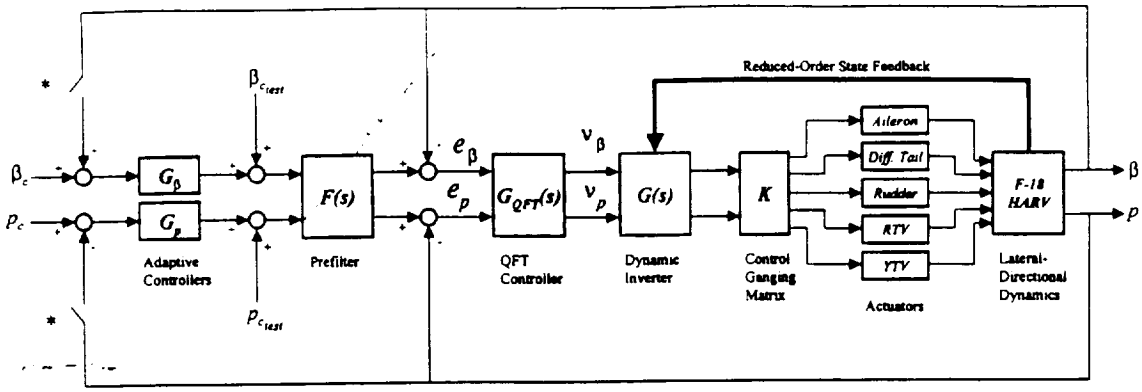


*Switces open before Adaptive Controllers obtained and Adaptive Controllers = unity

Figure 2 Flight Control System

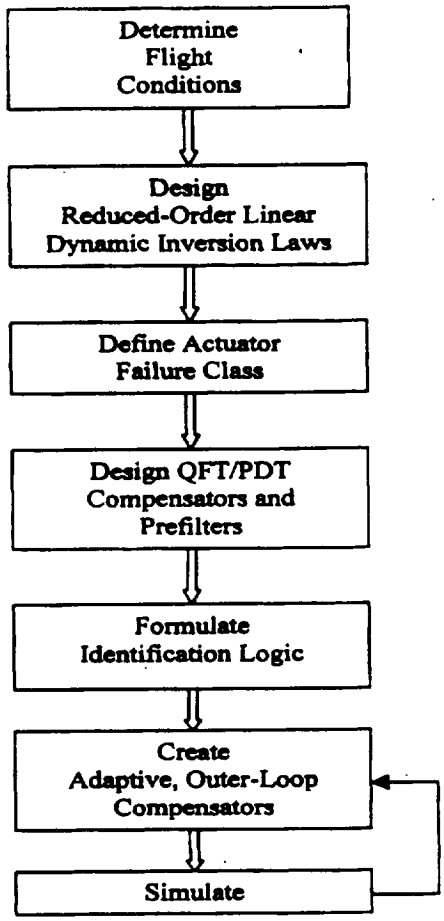


Figure 3 Steps in Design Methodology

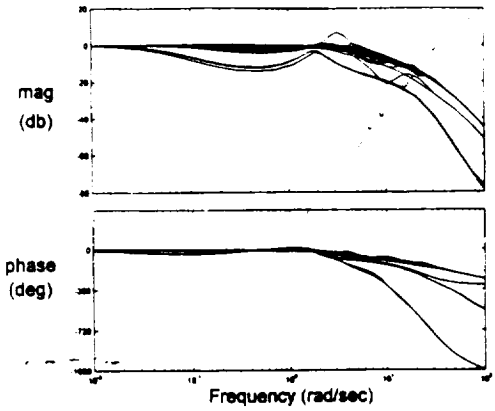


Figure 4 β/βc Transfer Functions with Failures

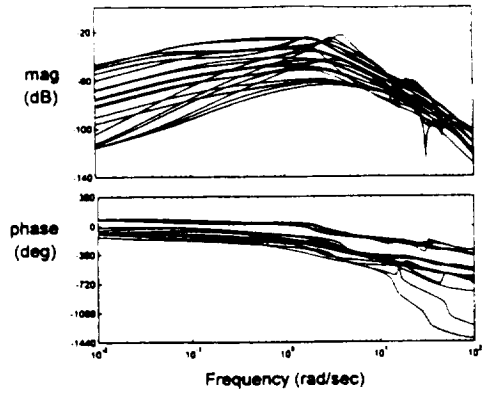


Figure 7 β/pc Transfer Functions with Failures

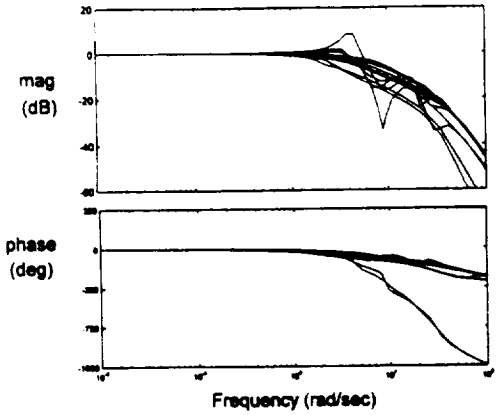


Figure 5 p/pc Transfer Functions with Failures

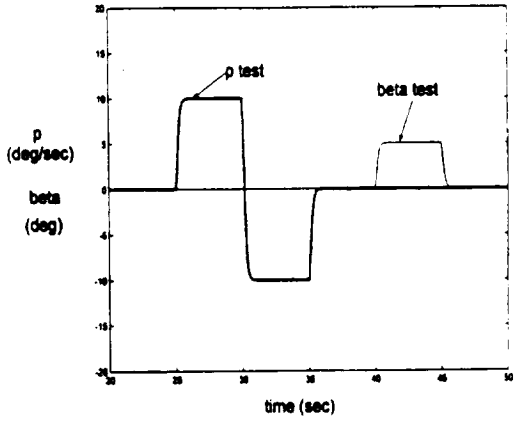


Figure 8 Test Inputs for Identification

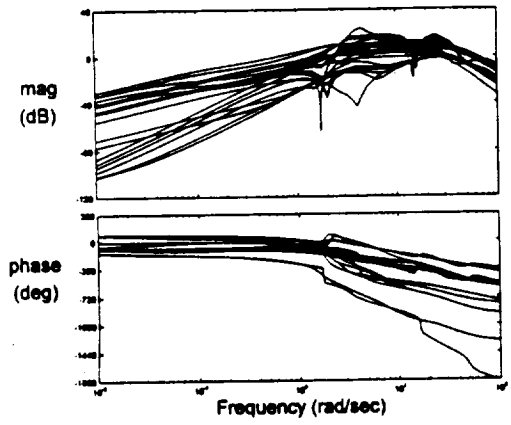


Figure 6 p/βc Transfer Functions with Failures

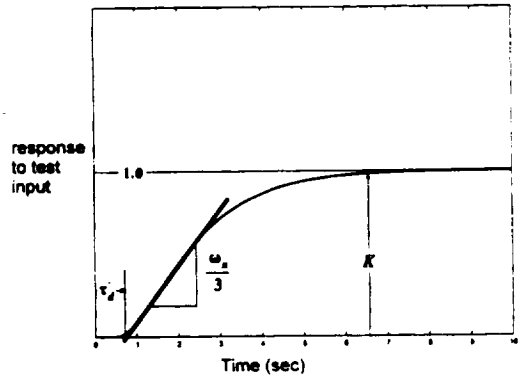


Figure 9 Identification of "Overdamped" Response

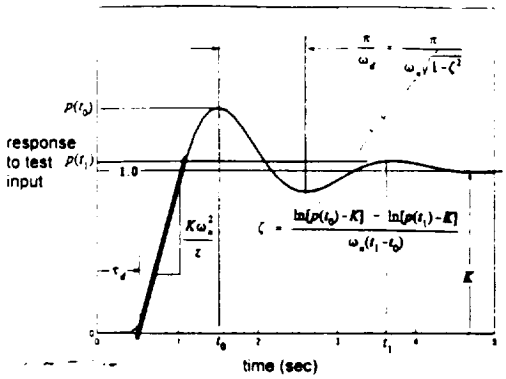


Figure 10 Identification of "Underdamped" Response

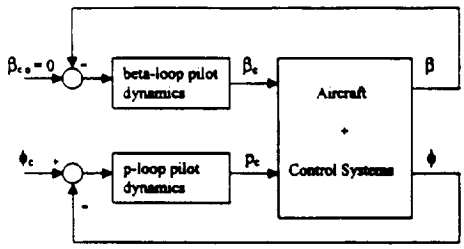


Figure 11 Pilot/Vehicle System for Computer Simulation

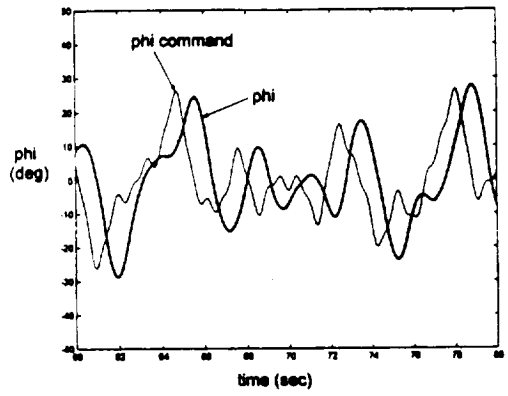


Figure 12 phi-loop Tracking Performance Nominal System

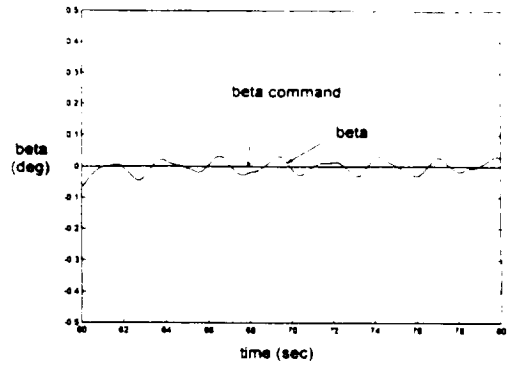


Figure 13 beta-loop Tracking Performance Nominal System

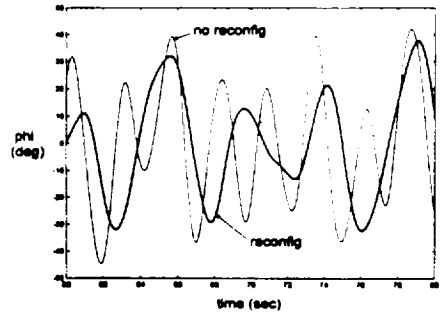


Figure 14 phi-loop Tracking Performance; Config. 9 with and without Reconfiguraion

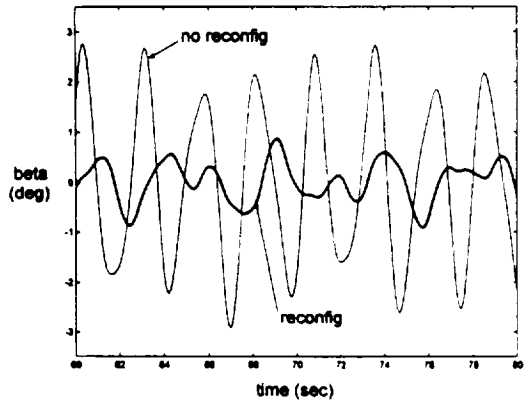


Figure 15 beta-loop Tracking Performance; Config. 9 with and without Reconfiguration

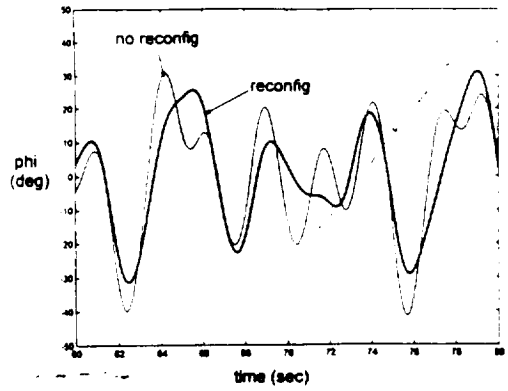


Figure 16 phi-loop Tracking Performance; Config. 31 with and without Reconfiguration

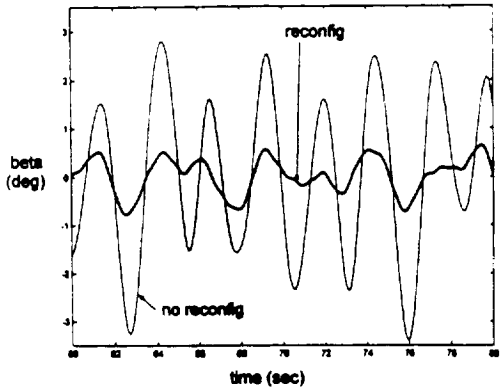


Figure 17 beta-loop Tracking Performance; Config. 31 with and without Reconfiguration

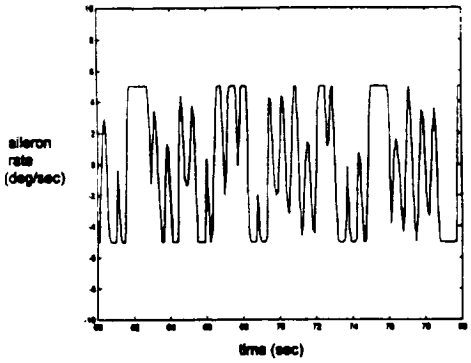


Figure 18 Aileron Actuator Rate Limiting; Config. 31 After Reconfiguration

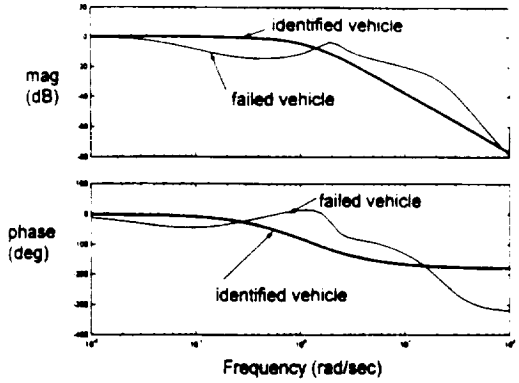


Figure 19 Comparison of Failed and Identified Vehicle Dynamics; beta loop, Linear

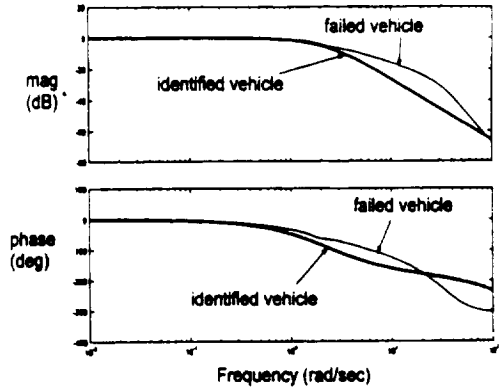


Figure 20 Comparison of Failed and Identified Vehicle Dynamics; p loop, Linear